

Comparative Studies of a Single Cell and a Stack of Direct Methanol Fuel Cells

Songki Lee***, Daejin Kim*, Jaeyoung Lee*, Sung Taik Chung** and Heung Yong Ha*†

*Fuel Cell Research Center, Korea Institute of Science and Technology, Seoul 136-791, Korea

**Department of Chemical Engineering, Inha University, Incheon 402-751, Korea

(Received 11 October 2004 • accepted 28 February 2005)

Abstract—Comparative studies have been conducted to observe the characteristics of a single cell and a stack of direct methanol fuel cells (DMFC) at ambient conditions. The maximum power density of a single cell was about 70 mW/cm² at 2 M methanol (CH₃OH) of 3.75 cc/min and dry air of 250 cc/min at room temperature and atmospheric pressure. In a stack, on the other hand, the maximum power density of the stack was 85 mW/cm² which was about a 20% higher value. This could be attributed to higher internal temperature than that of the single cell: the temperature of single cell increased up to 35 °C, while the highest temperature of the stack was 69 °C. This is because the cell temperature in DMFC was autonomously increased by exothermal reaction such as chemical oxidation of CH₃OH and oxygen reduction. The temperature was strongly dependent on the number of unit cells in a stack and the amount of electric load applied. In DMFC stacks, the performance of an individual cell showed uneven distribution when the electric load was increased and it was mostly influenced by different local concentration of reactants and non-uniform temperature.

Key words: DMFC, Single Cell, Stack, Durability, Temperature Distribution

INTRODUCTION

Of late, fuel cells have become a central focus of interest and leading car and power companies are making large scale investments in fuel cell systems. Fuel cells are set to provide electrical vehicles, small and large scale power stations, and even portable electrical applications such as laptops and mobile phones, with electrical power in a manner that is more efficient and more environmentally friendly than ever before [Carrette et al., 2001; McNicol et al., 2001]. In particular, direct methanol fuel cells (DMFCs) have been considered for use in very small to mid-sized applications due to their high electrical efficiency, long life-time, and low poisonous emissions [Carrette et al., 2001; Scott et al., 1999; Savadogo et al., 1998; Kim et al., 2004]. In the operation of DMFCs, there are several problems to be solved for the commercialization of DMFC. First, some of methanol diffuses through the polymer electrolyte membrane from the anode to the cathode - a phenomenon called methanol crossover that reduces cathode performance and fuel efficiency. Second, water loss and water recycling in DMFCs affect the complexity, volume and weight of the system and become of greater concern as the size of the DMFC decreases [Blum et al., 2003]. Another major problem in the use of DMFCs is the loss of water due to electromigration of water from the anode side to the cathode side [Zawodzinski et al., 1993; Ren et al., 2001] for individual membranes. Most of this water exits the cathode in the form of small droplets [Ren et al., 2001] and some water evaporates. Lastly, as Amphlett et al. [2001] presented in their study, the effect of temperature on DMFC performance was as expected. The maximum power density at 95 °C was approximately 50% greater than at 70 °C and much larger than at room temperature. The performance at the higher temperature was generally more stable and the appropriate cell temperature was

mostly controlled in order to get highest power density of the cell. Also, Scott et al. [Scott et al., 1999; Argyropoulos et al., 1999] presented that cell temperature influenced limiting current density of the cell. In the commercialization of the DMFC, all assistant components such as methanol fuel supplying devices, heating parts, blowers etc., must be minimized or not be used in order to decrease the volume and the weight and to increase energy efficiency of DMFC.

In this paper, we have investigated the characteristics of DMFC by comparing the performance and temperature change in a single cell and an 8-cell stack at various operation conditions.

EXPERIMENTAL

Cathode catalyst used was unsupported Pt black (E-TEK) and catalyst ink was prepared by dispersing appropriate amounts of catalyst in deionized water and isopropyl alcohol (IPA) with 5% Nafion® solution (1100 EW, DuPont). Anode catalyst used for methanol electro-oxidation was Pt-Ru black (E-TEK) and catalyst ink was prepared by the same method with the cathode ink. Complete catalyst ink was coated on a gas diffusion layer/carbon cloth (TGPH-060, Toray) with geometric area of 35 cm². Then, additional ionomer solution was sprayed onto the catalyst layer of each electrode in order to decrease the contact resistance with polymer electrolyte membrane (Nafion® 117, DuPont). The catalyst (Pt or PtRu) loading was 5 mg/cm² in each electrode and the total ionomer, including additional ionomer, loading was 10 wt% to catalyst for the cathode and 15 wt% to catalyst for the anode. A pair of electrodes (cathode and anode) was hot-pressed on both sides of the polymer electrolyte membrane at a temperature of 140 °C and with a pressure of 80 kg/cm² for 150 sec.

All experiments including electrochemical measurements were conducted with cells that consisted of MEAs sandwiched between two graphite flow field plates. Serpentine structure of graphite plate was used in order to guarantee homogeneous distribution of meth-

*To whom correspondence should be addressed.

E-mail: hyha@kist.re.kr

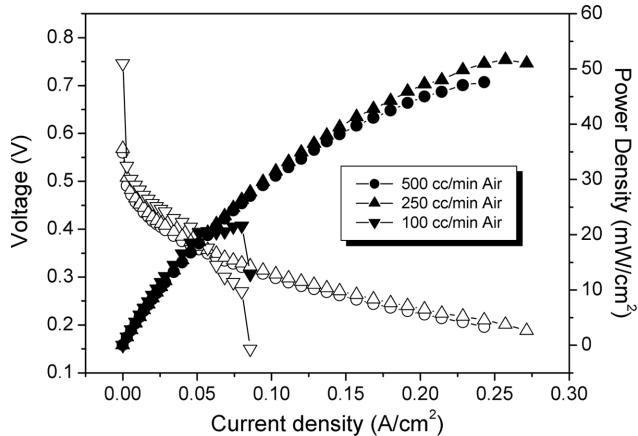


Fig. 1. Single cell performance with varying dry air flow rate at 2 M MeOH with 7.5 cc/min. Operation temperature = ca. 30 °C.

anol and air over the reaction surface area as well as removal of products such as carbon dioxide and water from the cell [Tüber et al., 2003, 2004]. In all the experiments operated in a fuel cell mode, various concentrations of methanol solution were pumped through the anode side and dry air to the cathode side. The cell performance was measured at autonomous increase of temperature and ambient pressure. Current-voltage curves were measured galvanostatically by using an electronic load (EL-500P, Daegil Electronics), and the temperature of single cell and individual cell of the stack was continuously recorded. Impedance spectra were measured at different methanol concentration by using a potentiostat and galvanostat/log-in amplifier (Zahner IM6), and the frequency range investigated reached from 1 kHz to 50 mHz with 10 points per decade.

RESULTS AND DISCUSSION

Fig. 1 shows the effect of air flow rate on the cell performance. The air stoichiometry (λ) of air flow rate of 100, 250 and 500 cc/min is 0.60, 1.50 and 3.0 at 250 mA/cm², respectively. It can be seen that at the air flow rates of 250 and 500 cc/min, the performances were almost same while at the lower flow rate of 100 cc/min of which the air stoichiometry was 1.0 only at 150 mA/cm² the voltage dropped rapidly above the current of 100 mA/cm² because of insufficient oxygen supply. Since the single cell was operated at room temperature, the internal temperature of the cell could be easily affected by the air flow rate. And thus, the slightly lower performance at 500 cc/min than at 250 cc/min might be attributed to the lower temperature at the higher air flow rate.

Figs. 2(a) and 2(b) show single cell performances with different CH_3OH feeding rates and concentrations, respectively. In Fig. 2(a), we find optimal methanol flow rate of 3.75 cc/min and its stoichiometry (λ) at 300 mA/cm² is 7.2. The slower feeding of methanol results in inappropriate supply of reactants even if the stoichiometry (λ) is larger than 4.0. This may be due to slow diffusion rate of methanol in the liquid phase. On the other hand, faster flow rate appears to induce lower cell temperature and more methanol crossover to decrease the performance. Fig. 2(b) shows that power density is strongly dependent on CH_3OH concentration. Below 1.0 M meth-

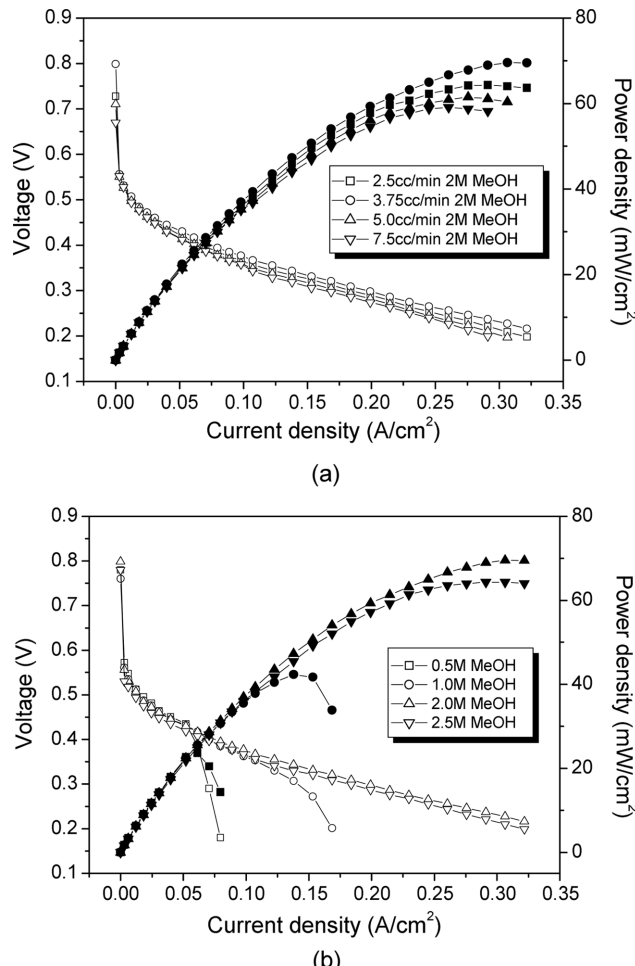


Fig. 2. Single cell performance with varying (a) methanol flow rate of 2 M MeOH and (b) MeOH concentration with applying flow rate of 3.75 cc/min. Dry air = 250 cc/min.

anol concentration, there is mass transport limitation, while more methanol would diffuse into the cathode at 2.5 M to increase the overpotential of the cathode.

Analyzing the experimental observations from Figs. 1 and 2, optimal conditions for production of maximum power density in a single cell are (i) 2.0 M methanol solution at 3.75 cc/min and (ii) air flow rate of 250 cc/min. Under optimum conditions of the system, a maximum power density of the cell is about 70 mW/cm² at room temperature and atmospheric pressure.

In order to understand the data in Fig. 1, the electrochemical impedance spectra of the cell were measured, and Nyquist plots obtained at different methanol concentration are shown in Fig. 3. All impedance plots exhibit clock-wise loop indicating dynamically stable stationary mode. Lower methanol concentration induces the impedance to increase and it is in good agreement with lower cell performance observation of Fig. 1(a).

One of the critical issues in all kinds of fuel cell systems is temperature control. In DMFC, however, temperature control is not as difficult as in other types of fuel cells that release large amount of heat or operate at high temperatures because the DMFC operates at low temperature and produces a relatively small amount of heat. Moreover, in the DMFC, an aqueous methanol solution is used as a

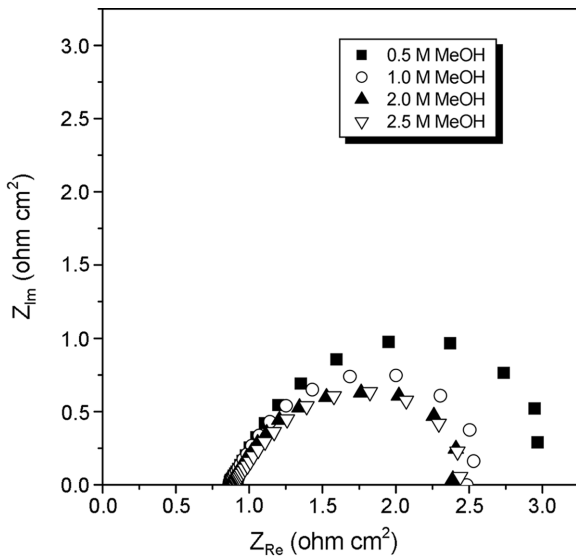


Fig. 3. Single cell impedance of the anode with varying MeOH concentration. Methanol flow rate=3.75 cc/min, hydrogen flow rate=500 cc/min. Applied anodic voltage=0.5 V.

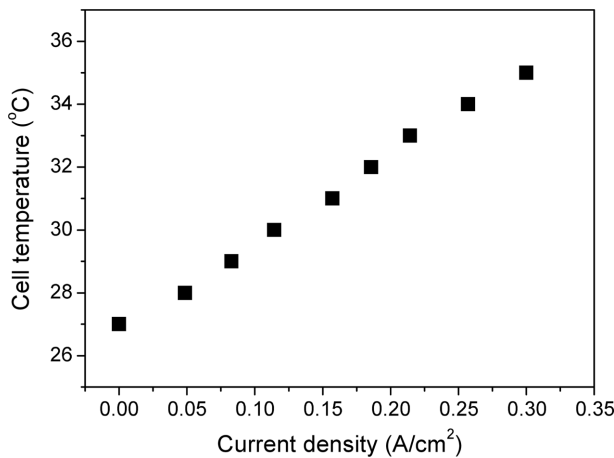


Fig. 4. Change in cell temperature with increasing current density under 3.75 cc/min 2 M MeOH and 250 cc/min dry air conditions.

reactant and thus it could dissipate large amount of heat that is produced by electrochemical reactions. However, DMFC performance is very dependent on temperature and thus the system should be maintained at an appropriate temperature. In order to understand the temperature change in a single cell system, cell temperature was monitored with varying electric load as shown in Fig. 4. The cell temperature increased almost linearly with increasing current density at a heating rate of $28\text{ }^{\circ}\text{C}/(\text{A}/\text{cm}^2)$ and marked $35\text{ }^{\circ}\text{C}$ at the limiting current density of $300\text{ mA}/\text{cm}^2$. Thermodynamically, cell temperature could be increased by two main exothermal reactions such as chemical oxidation of crossover methanol and oxygen reduction on the cathode. Thermal contribution by oxidation of crossover methanol could be estimated from temperature change at open circuit. Under the given conditions of 2 M methanol of $3.5\text{ cc}/\text{min}$ and dry air of $250\text{ cc}/\text{min}$ at room temperature, the temperature increment was only $2\text{ }^{\circ}\text{C}$ at open circuit. This small temperature change is be-

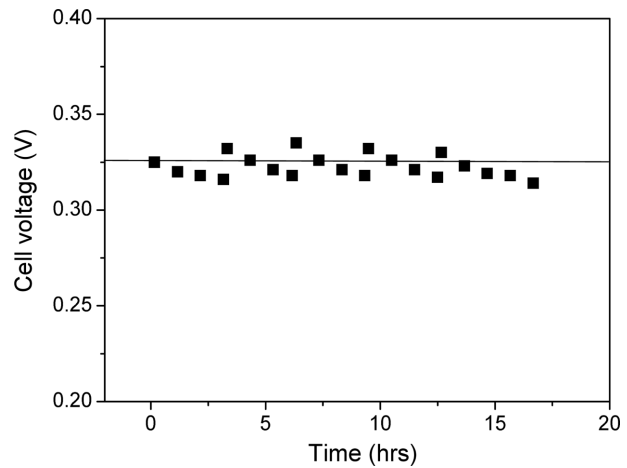


Fig. 5. The distribution of single cell voltage at 3.5 A for long term.

cause the methanol feed concentration is low and the heat produced by oxidation of crossover methanol got dissipated by air that is fed to the cathode. When an electric load was applied to the cell, the temperature was further increased in proportion to the amount of load and reached $35\text{ }^{\circ}\text{C}$ at $300\text{ mA}/\text{cm}^2$. The cell temperature is mostly affected by the area of the electrode, the number of unit cells in a stack and the amount of electric load. This will be shown in a later section that deals with a stack with 8 unit cells.

In this study, a continuous operation was conducted to observe the change in the performance. Fig. 5 shows the result of single cell performance with a load of 3.5 A ($100\text{ mA}/\text{cm}^2$) at room temperature. The cell voltage does not sustain its initial value, but declines gradually. When the cell was shut down after 3 hours of operation and resumed its reaction again after an hour, it recovered its initial performance. We could affirm this phenomenon by repeated shutdowns and operations as shown in this figure. The temporary deactivation might be caused by accumulation of water in the cathode side which diffused from anode by electro-osmotic drag and concentration gradient and accumulation of carbon dioxide that was produced by electrochemical oxidation of methanol in the anode.

Based on single cell study, we designed and manufactured a stack of which the graphite plates had the same flow field as that used in the single cell experiments. In general, it is not easy to construct a reliable stack, and moreover to get a comparable performance to that of single cells because of leakage and intermixing of reactants, uneven distribution of reactants throughout the unit cells, increased ohmic resistance and deviation in the activity of MEAs used in the stack.

Fig. 6 is a photograph of the main body of the DMFC stack consisting of 8 unit cells with an active electrode area of 35 cm^2 per cell. The reactants, methanol solution to the anode and air to the cathode, were fed at opposite side of the stack to make a counter-flow system because the counter-flow system was known to present better performance compared with the co-flow system.

Fig. 7(a) shows the power output of the stack at different methanol concentrations. As in the case of the single cell system, the best performance was achieved at a methanol concentration of 2 M with a total power of 24 W . Fig. 7(b) shows the cell performance redrawn in terms of power density. The maximum power density is $85\text{ mW}/$

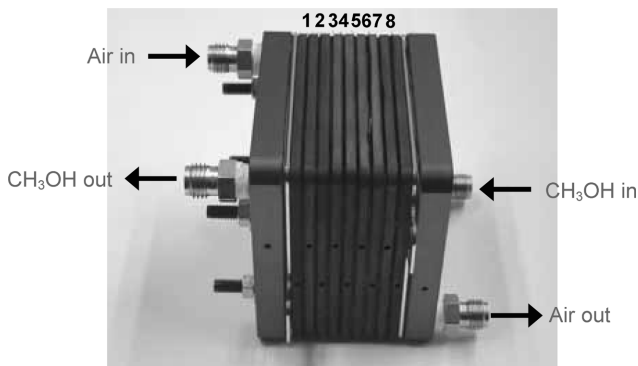


Fig. 6. A photograph of a DMFC stack.

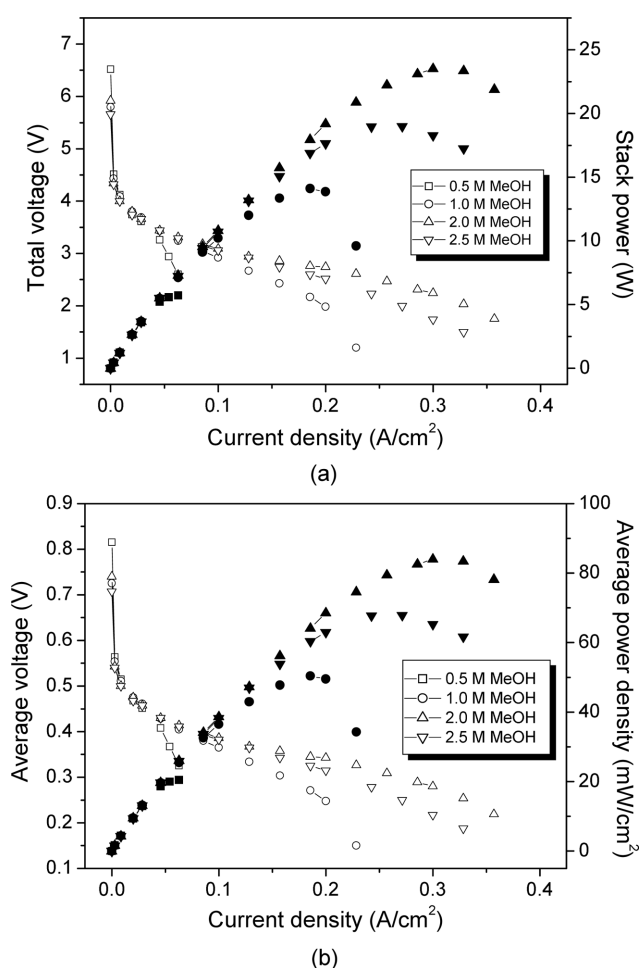


Fig. 7. (a) Stack power and (b) average power density with varying MeOH concentrations at 20 cc/min MeOH solution and 6 slm dry air.

cm² and it is *ca.* 20% higher than that of the single cell shown in Fig. 1. The higher power density of the stack is attributed to higher internal temperature than that of the single cell. More discussion on the stack temperature will be given in a later section.

Figs. 8(a) and (b) show stack performances depending on flow rates of methanol and of dry air, respectively. In Fig. 8(a), I-V curves are exhibited at different flow rates of the 2 M metha-

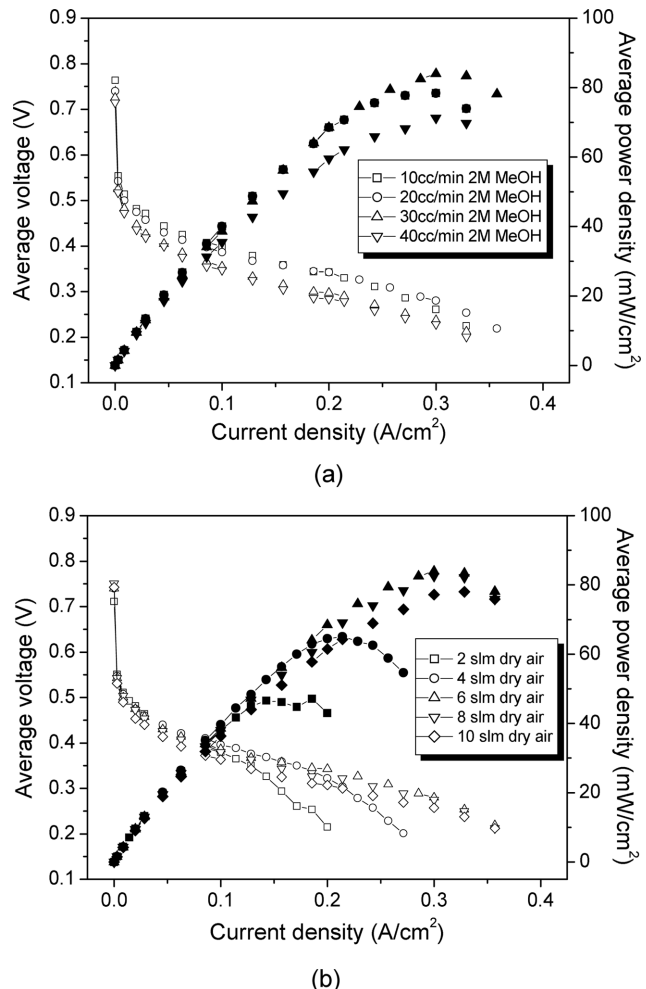


Fig. 8. (a) average power density of the stack with varying MeOH flow rate at 6 slm dry air. (b) average power density of the stack with varying dry air flow rate at 20 cc/min 2 M MeOH.

nol solution while flowing dry air of 6 L/min at room temperature. As in the case of the single cell the stack performance was affected by methanol flow rate, and it passed through a maximum value at a flow rate of 20 cc/min. However, the flow rate appeared not to be directly proportional to the number of unit cells. That is, the maximum power of the single cell was obtained at a flow rate of 3.75 cc/min, but for the stack with 8 unit cells the optimum flow rate was only 20 cc/min, lower than 30 cc/min. Even the 10 cc/min methanol feed showed a performance comparable to 30 cc/min feed. The reason for maximum performance attained at a lower methanol flow rate compared with the single cell is not clear. We assume that it might be related to the rate of methanol crossover that deactivates the cell performance by forming a mixed potential at the cathode. This deactivation could be more prominent in the stack in which the internal temperature is higher than that of the single cell because methanol crossover is accelerated with increasing methanol flow rate and temperature.

Air supply in the stack is another important issue in the DMFC system because the parasitic power loss should be minimized to enhance the energy density of the portable power system. A set of

experiments was conducted to find an optimum air flow rate. Under the given conditions, the maximum power was obtained at an air flow rate of 6 L/min as shown in Fig. 8(b). Considering the optimum air flow rate is 250 cc/min for the single cell (see Fig. 2), 6 slm is much higher than the calculated value of 2 slm ($0.25 \times 8 = 2$ L/min). In general, the higher flow rate is desirable to get a uniform gas distribution all over the stack and to increase the oxygen concentration in the electrodes unless the temperature is decreased to decrease the stack performance by the cooling effect of the excess air. Therefore, it is speculated higher temperature of the stack tolerates the larger air flow rate to get the higher power output.

Fig. 9 presents distribution of cell voltage in the stack at different current densities. The voltage distribution is uniform all over the unit cells at OCV and current densities lower than 7 A (200 mA/cm^2). This shows that the cells were well assembled without leakages and intermixing of the reactants in the stack. However, as the current was increased higher than 10.5 A (300 mA/cm^2), the discrepancy among the cells was exaggerated and the cells of 7 and 8 exhibited remarkably low voltages. The uneven voltage distribution at high current might be due to difference in MEA performances,

uneven supply of the reactants and large contact resistances between adjacent cells.

As mentioned above, cell temperature is of great significance in DMFC operation since it directly influences the reaction rate of the cell. Fig. 10 shows temperature change of the DMFC stack with varying current density at different methanol concentrations. At open circuit state, stack temperature increased from 25 to 42 °C with increasing methanol feed concentration from 0.5 to 2.5 M, reflecting the dependence of methanol crossover on methanol concentration of the feed. For instance, at 2.0 M the temperature rose to 39 °C, much higher than that (27 °C) of the single cell (Fig. 4). The large increment in stack temperature at open circuit is presumably because the stack with 8 unit cells could preserve heat better than the single cell. Upon bringing about electrochemical reactions by applying electric load the stack temperature increased further with increasing the current and the methanol feed concentration. With a 2 M methanol solution, the temperature increased at a rate of 73 °C/(A/cm²) and reached 63 °C at a load of 300 mA/cm². This temperature is high enough to produce a full DMFC performance without external heating.

Fig. 11 presents the temperature distribution over the stack at different electric loads. Temperatures were lower at the outer cells and higher at the central ones probably because of insulation effect and heat dissipation by the reactants that were fed at room temperature. The lowest temperatures were observed at cell 1 at which the methanol inlet port is located. The cold methanol feed entering the stack was likely to drop temperature of the first cell. The highest temperature was recorded at cell 6 and it was 63 °C at a load of 300 mA/cm².

As shown previously, the temperature of DMFC increased up to 63 °C by the heat released during electrochemical reactions in the absence of external heating. Temperature increment depends on the size and the number of cells in the stack and, moreover, it varies with an electric load applied. Though a higher temperature is required to get higher performance, the temperature should be controlled properly considering the applications, portability and durability of the DMFC systems.

Fig. 12 shows the change in stack voltage at a load of 3.5 A (100

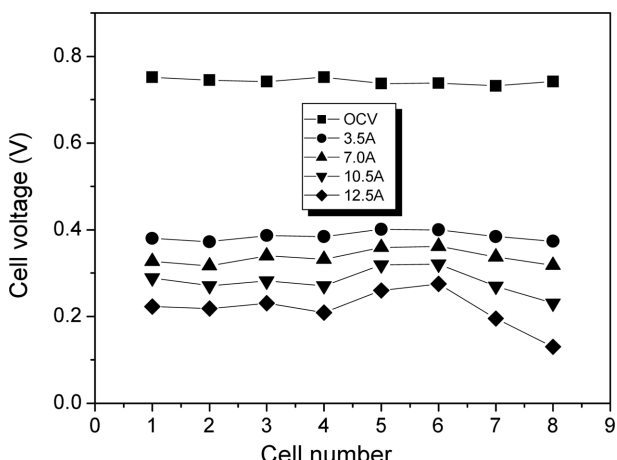


Fig. 9. The distribution of cell voltage of the DMFC stack under at various currents.

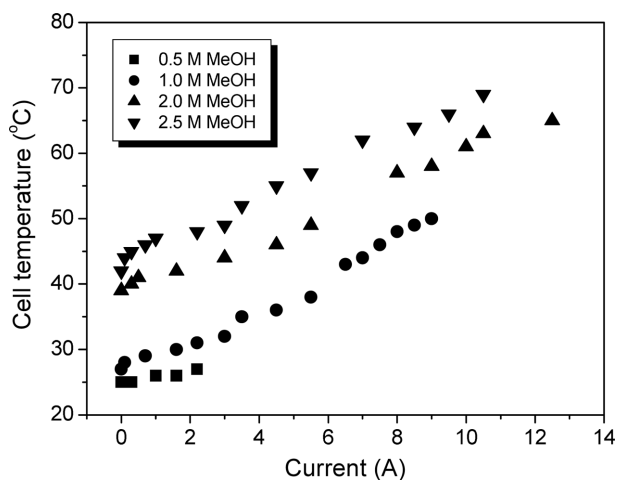


Fig. 10. The distribution of stack temperature with varying MeOH concentration with increasing current density.

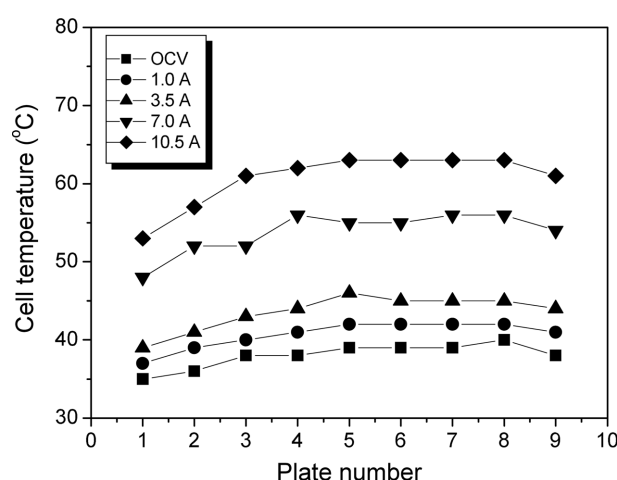


Fig. 11. Stack temperature distribution according to graphite plate number.

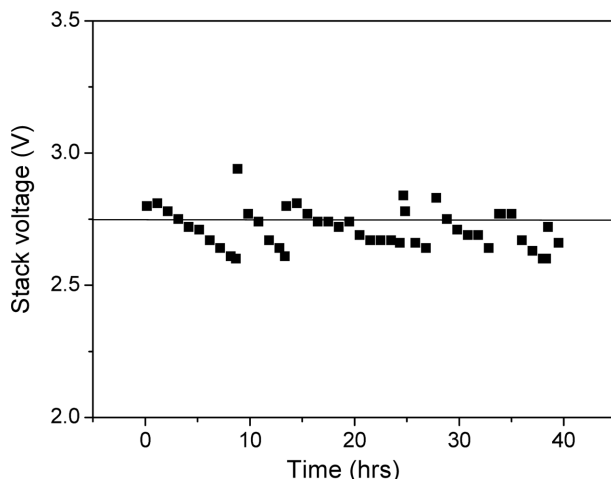


Fig. 12. The change in stack voltage at a load of 3.5 A (100 mA/cm^2) during the continuous operation under the conditions of 2 M methanol solution of 3.5 cc/min, dry air of 6 slm.

mA/cm^2) during continuous operation under the conditions of 2 M methanol solution of 3.5 ml/min, dry air of 6 slm, room temperature and atmospheric pressure. As in the case of the single cell, the stack voltage declined gradually with time on-stream and it needed a shut-down every 10 hours to recover its initial performance. The temporary deactivation might be caused by accumulation of water in the cathode side and accumulation of carbon dioxide in the anode side that was produced by electrochemical oxidation of methanol as mentioned previously.

CONCLUSION

The internal temperature of the cell autonomously increased much above the room temperature without applying any external heating in the operation of direct methanol fuel cell systems. In a single cell with active area of 35 cm^2 , the temperature of the cell increased to 35°C and it showed power density of 70 mW/cm^2 at 300 mA/cm^2 . On the other hand, we observed cell temperature of ca. 70°C at 300 mA/cm^2 in the case of a stack consisting of 8 unit cells with an active area of 35 cm^2 per cell. Analyzing experimental observations of single cell and stacks, we concluded that cell temperature was strongly dependent on the area of the electrode, the number of unit cells in a stack, and the amount of electric load. In other words, autonomous temperature increase of an individual cell was due to two exothermal reactions, such as chemical reaction of crossover methanol and oxygen reduction at the cathode. In the stack, maximum power density was 85 mW/cm^2 and it was 20% higher than that of the single cell. Cell temperature was evenly distributed at low current, while inhomogeneity became obvious with increasing current. From these experimental observations, it is speculated that the internal temperature of the DMFC power generation system having a large num-

ber of unit cells could increase higher than 80°C and thus appropriate temperature control system may be required to avoid overheating and ensure its long-term stability.

ACKNOWLEDGMENTS

This work was supported by INHA UNIVERSITY Research Grant (INHA-22741-01).

REFERENCES

- Amphlett, J. C., Peppley, B. A., Halliop, E. and Sadiq, A., "The Effect of Anode Flow Characteristics and Temperature on the Performance of a Direct Methanol Fuel Cell," *J. Power Sources*, **96**, 204 (2001).
- Argyropoulos, P., Scott, K. and Taama, W. M., "Engineering Aspects of the Direct Methanol Fuel Cell System," *J. Power Sources*, **79**, 43 (1999).
- Blum, A., Duvdevani, T., Philosoph, M., Rudoy, N. and Peled, E., "Water-neutral Micro Direct-methanol Fuel Cell (DMFC) for Portable Applications," *J. Power Sources*, **117**, 22 (2003).
- Carrette, L., Friedrich, K. A. and Stimming, U., "Anodenstruktur Für Interne Methanreformierung," *Fuel Cells*, **1**, 5 (2001).
- Kim, D., Cho, E. A., Hong, S.-A., Oh, I.-H. and Ha, H. Y., "Recent Progress in Passive Direct Methanol Fuel Cells at KIST," *J. Power Sources*, **130**, 172 (2004).
- McNicol, B. D., Rand, D. A. J. and Williams, K. R., "Fuel Cells for Road Transportation Purposes - Yes or No?," *J. Power Sources*, **100**, 47 (2001).
- Ren, X. and Gottesfeld, S., "Electro-osmotic Drag of Water in Poly(per-fluorosulfonic acid) Membranes," *J. Electrochem. Soc.*, **148**, A87 (2001).
- Savadogo, O., "Hydrogen/Oxygen Polymer Electrolyte Membrane Fuel Cell (PEMFC) Based on Acid-doped Polybenzimidazole (PBI)," *New Mater. Electrochem. Syst.*, **1**, 47 (1998).
- Scott, K., Taama, W. M., Argyropoulos, P. and Sundmacher, K., "The Impact of Mass Transport and Methanol Crossover on the Direct Methanol Fuel Cell," *J. Power Sources*, **83**, 204 (1999).
- Scott, K., Taama, W. M., Kramer, S. and Argyropoulos, P., "Limiting Current Behaviour of the Direct Methanol Fuel Cell," *Electrochim. Acta*, **45**, 945 (1999).
- Tüber, K., Oedegaard, A., Hermann, M. and Hebling, C., "Investigation of Fractal Flow-fields in Portable Proton Exchange Membrane and Direct Methanol Fuel Cells," *J. Power Sources*, **131**, 175 (2004).
- Tüber, K., Póczka, D. and Hebling, C., "Visualization of Water Buildup in the Cathode of a Transparent PEM Fuel Cell," *J. Power Sources*, **124**, 403 (2003).
- Zawodzinski, T. A., Derouin, C., Radzinski, S., Sherman, R. J., Smith, V. T., Springer, T. E. and Gottesfeld, S., "Water Uptake by and Transport through Nafion 117 Membranes," *J. Electrochem. Soc.*, **140**, 1041 (1993).